

IMECE2011-64174

## BIO-INSPIRED ROBOTIC COWNOSE RAY PROPELLED BY ELECTROACTIVE POLYMER PECTORAL FIN

**Zheng Chen\***

Department of Mechanical & Aerospace Engineering  
University of Virginia  
Charlottesville, Virginia 22904  
Email address: zc7u@virginia.edu

**Tae I. Um**

Department of Mechanical & Aerospace Engineering  
University of Virginia  
Charlottesville, Virginia 22904  
Email address: tiu2f@virginia.edu

**Jianzhong Zhu**

Department of Mechanical & Aerospace Engineering  
University of Virginia  
Charlottesville, Virginia 22904  
Email address: jz8n@virginia.edu

**Hilary Bart-Smith**

Department of Mechanical & Aerospace Engineering  
University of Virginia  
Charlottesville, Virginia 22904  
Email address: hb8h@virginia.edu

### ABSTRACT

*The cownose ray (*Rhinoptera bonasus*) demonstrates excellent swimming capabilities; generating highly efficient thrust via flapping of dorsally flattened pectoral fins. In this paper, we present a bio-inspired and free swimming robot that mimics the swimming behavior of the cownose ray. The robot has two artificial pectoral fins to generate thrust through a twisted flapping motion. Each artificial pectoral fin consists of one ionic polymer-metal composite (IPMC) as artificial muscle in the leading edge and a passive PDMS membrane in the trailing edge. By applying voltage signal to the IPMC, the passive PDMS membrane follows the bending of IPMC with a phase delay, which leads to a twist angle on the fin. The characterization results have shown that the pectoral fin was able to generate up to 40% tip deflection and 10° twist angle with less than 1 Watt power consumption. A bio-inspired rigid body was designed using Computerized Axial Tomography (CT Scan) data of the cownose ray body and printed using a 3-dimensional printer. A light and compact on-board control unit with a lithium ion polymer battery has been developed for the free swimming robot. Experimental results have shown that the robot swam at 0.034 BL/S.*

### INTRODUCTION

The cownose ray (*Rhinoptera bonasus*, shown in Fig. 1) demonstrates excellent swimming capabilities; generating highly efficient thrust via flapping of dorsally flattened pectoral fins [1]. Many efforts have been directed towards building a bio-inspired pectoral fin structure to mimic the swimming behavior of the ray, such as electric motor actuated rigid plates [2] and tensegrity structures [3]. Due to size limitations of the electric motors and tensegrity structures, they are not suitable for small scale robots (on the order of 5-10 cm) [4–6]. A bio-inspired actuating material, which is lightweight, compliant, resilient, and capable of generating 3D deformation with low power consumption, is highly desirable in constructing a free swimming and small scale robotic cownose ray.

Electroactive polymers (EAPs), also known as *artificial muscles*, can generate large deflections under electrical stimulus [7]. Ionic polymer-metal composites (IPMCs) are one category of ionic EAPs [8], which can work well under a low actuation voltage (1 to 2 Volts) in a sodium salt water environment. An IPMC consists of one ion exchange membrane, such as Nafion (DuPont), coated with two novel metal electrodes [9]. When the IPMC is hydrated, the positive ions in the Nafion polymer, such

\*Address all correspondence to this author.



**FIGURE 1.** Bio-inspiration: Atlantic cownose ray (courtesy of [www.elasmodiver.com](http://www.elasmodiver.com)).

as sodium and calcium ions, can be transported to the cathode side under an electric field, whereas the negative ions are permanently fixed to the carbon chain. The ion transportation introduces swelling in the cathode side and shrinking in the anode side, which leads to the bending motion of the IPMC. Figure 2 illustrates the actuation mechanism of IPMC.

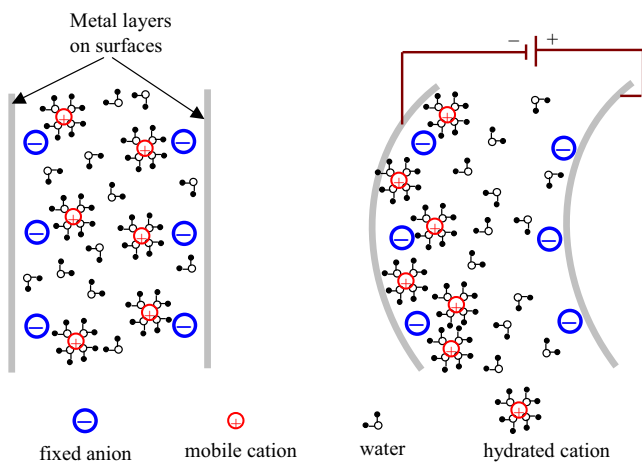


**FIGURE 2.** Actuation mechanism of IPMC (cross-section view) [8].

IPMC has been used as a caudal fin in bio-inspired robotic fishes [4, 10], where the propulsive fin mimics the bending motion observed in many biological fishes. In the propulsion mechanism of rays, 3-dimensional kinematic motions on the pectoral fin play an important role in generating highly efficient propulsion and maneuvering [1]. In order to obtain an actuating mem-

brane capable of generating 3D deformation, some lithography-based [11] and surface machining-based approaches have been explored to pattern the electrodes of the IPMC in order to create active and passive areas in a Nafion membrane. By individually controlling the bending of each active area, some 3D deformations of the membrane have been demonstrated. However, the stiffness of the Nafion in the passive area limited its capability of generating twisting motions. Anton *et al* developed pectoral fins for ray-like underwater robot by assembling separated IPMC beams with a latex foil [12]. But their robot did not achieve free swimming capability because of high power consumption and low propulsion efficiency. In our previous work, an assembly-based fabrication technique was developed to integrate IPMC actuators into an artificial pectoral fin design [13]. The fin was fabricated by bonding four IPMC beams with a thin membrane of polydimethylsiloxane (PDMS). A free-swimming robotic manta ray was developed based on that pectoral fin. However, the undulation motion was not demonstrated in the free swimming test because of the complicated on-board control strategy.

In this study, a bio-inspired and free swimming robotic cownose ray propelled by artificial pectoral fins has been successfully developed. The pectoral fin consists of one IPMC as artificial muscle in the leading edge and a passive PDMS membrane in the trailing edge. The overall shape of the fin mimics that of the biology. By applying voltage potential to the IPMC, the passive PDMS membrane follows the bending of IPMC with a phase delay, which causes a twist angle on the fin. The flapping motion coupled with a twist angle leads to the thrust generation. The fin has been characterized by some key factors as they are related to the function of the robot: tip deflection, twist angle, and power consumption. A bio-inspired rigid body has been designed using Computerized Axial Tomography (CT Scan) data of the cownose ray body and printed using a 3-dimensional printer. A light and compact on-board control unit with a lithium ion polymer battery has been used for generating control signal to the IPMC in the pectoral fin. Experimental results have shown that the robot is capable of free swimming.

The rest of this paper is organized in the following manner. Artificial pectoral fin fabrication will be described in the next section. Characterization of the fin will be discussed in the third section. The design of the robotic cownose ray is shown in the fourth section. Then the free swimming testing of the robot will be discussed in the fifth section where the snap shots of the swimming robot have shown. The conclusion and future work are discussed in the last section.

## FABRIACTION OF ARTIFICIAL PECTORAL FIN

The proposed artificial pectoral fin must be able to generate oscillatory motion with a twist angle observed in nature, while under hydrodynamic loads. In this paper, an artificial pectoral fin was fabricated by combining IPMC actuator with a PDMS

elastomer in a mold to create a predefined planform shape. The design of pectoral fin is shown in Fig. 3. The outline shape of the fin mimics that of the biological cownose ray. An IPMC beam is placed in the leading edge of the fin. The rest of the fin is composed by a PDMS passive membrane.

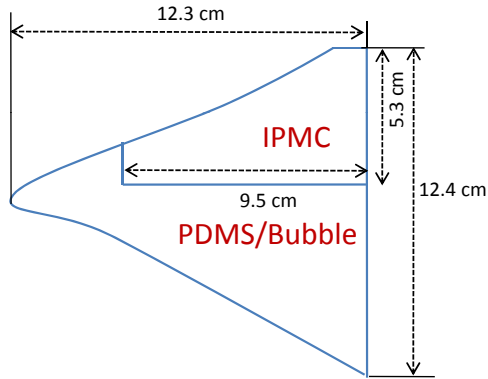


FIGURE 3. Artificial pectoral fin design.

The first step in creating the artificial pectoral fin is to fabricate the IPMC actuator. Many groups have developed different IPMC fabrication processes for various purposes [8, 14–16]. In our fabrication method, we followed most of the procedure outlined by K. Kim and M. Shahinpoor [14] but added multiple platinum plating processes to reduce the surface resistance of the electrodes [17]. A Nafion (Nafion™ N1110, DuPont) membrane was selected as the ion exchange membrane in IPMC. After the electroless plating processes, about 6  $\mu\text{m}$  thick platinum electrodes have been deposited on the Nafion surfaces with good polymer-metal adhesion. The sample was then submerged in a sodium solution (1 N) for one day to exchange  $\text{H}^+$  with  $\text{Na}^+$  to enhance the actuation performance of the IPMC.

After the IPMC has been fabricated, the next step is to bond the IPMC with a PDMS elastomer membrane. The PDMS bonding process is shown in Fig 4. First, two Delrin polymer (McMaster) molds were made using a CNC rapid milling machine (MDX-650, Roland). Each mold has two concaved areas to house PDMS passive membrane and IPMC actuator in the molding process. The thickness of PDMS membrane is 1 mm and thickness of IPMC is 280  $\mu\text{m}$ . Second, the IPMC was cut into the shape shown in Fig. 3. Third, 5% glass bubbles (Glass bubble K37, 3M Inc) were added into PDMS gel (Ecoflex 0030, Smooth-on Inc.) to gain a neutrally buoyant pectoral fin. To make it visible underwater, blue dye was added into the PDMS gel. Fourth, the IPMC and the PDMS gel were then clamped with the mold and the PDMS was cured at room temperature for 3 hours. Finally, the IPMC/PDMS artificial pectoral fin (Fig. 5) was removed from the mold.

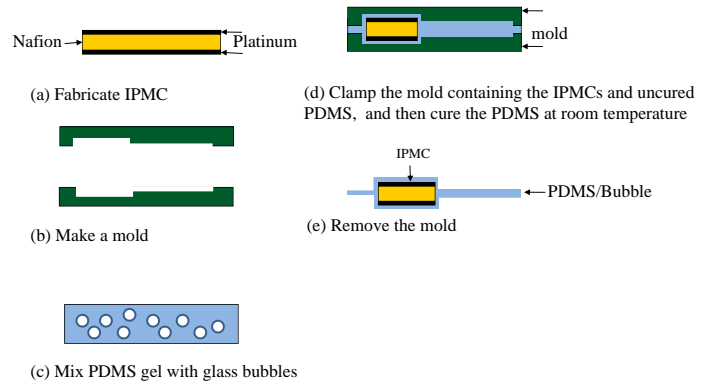


FIGURE 4. Fabrication process (cross-section view).

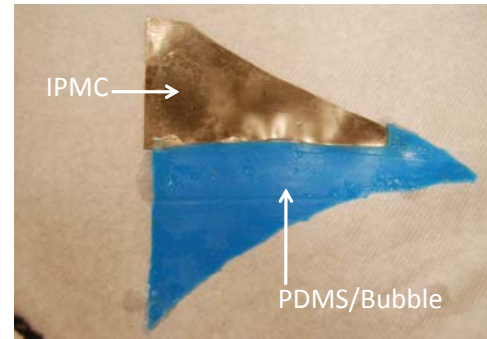


FIGURE 5. IPMC/PDMS artificial pectoral fin.

## CHARATERIZATION OF ARTIFICIAL PECTORAL FIN

The pectoral fin was characterized in terms of tip deflection, twist angle, and power consumption. These characteristics are useful in providing comparison data in the design of the bio-inspired robot. To characterize the actuating response of the pectoral fin, three testing points (A, B, C) are defined on the membrane (shown in Fig. 6).

### Tip deflection measurement

To measure the tip deflection, the fin was actuated in a transparent tank containing water. A laser sensor (OADM 2016441/S14F, Baumer Electric) was fixed outside of the tank to measure the bending displacement at point A. The tip deflection was normalized by dividing the bending displacement by the length at point A. Fig. 7 shows the tip deflection when a square wave actuation voltage (0.1 Hz, 4 V) was applied to the IPMC. It shows a peak-to-peak deflection of 40% of the spanwise dimension. One can achieve a larger deflection by applying a higher actuation voltage. But there is a limit to the size of voltage applied across the IPMC—anything greater than 6 V risks dielectric breakdown through the IPMC [8].

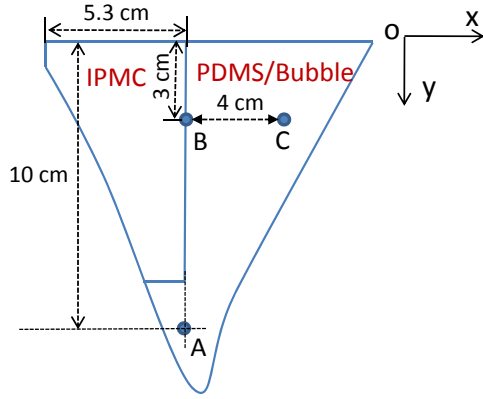


**FIGURE 6.** Testing points of the pectoral fin.

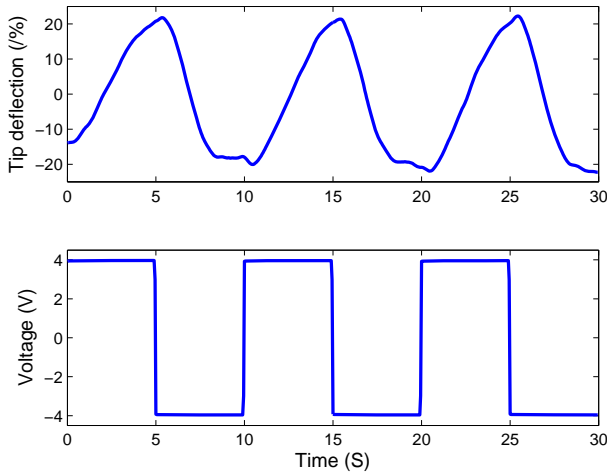


**FIGURE 7.** Tip deflection at point A under a square wave actuation voltage (0.1 Hz, 4 V).

To capture the Bode plot of the actuation dynamics of the fin, a series of sinusoidal actuation signals with an amplitude of 4 V and frequencies ranging from 0.1 Hz to 0.8 Hz were applied to the IPMC. The tip deflections at Point A and actuation voltage were measured. The magnitude and phase shift of the deflection over the actuation voltage were calculated. The Bode plot (Fig. 8) demonstrates that the actuation dynamics of the pectoral fin behaves as a low-pass filter with about 0.3 Hz cut-off frequency. This is to be expected as the ions in the IPMC cannot move very rapidly [18] and the hydrodynamic force acting on the fin dampens the high frequency vibration [19].

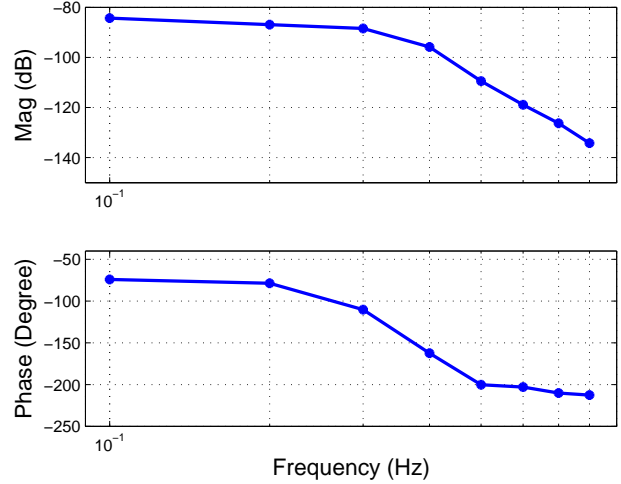


**FIGURE 8.** Bode plot of the actuation dynamics of the pectoral fin.

### Characterization of twisting motion

In order to characterization of the fin's 3D kinematics, two laser sensors (OADM 20I6441/S14F, Baumer Electric) were used to measure the bending displacements  $d_B$  and  $d_C$  at the point B and C, respectively. The twist angle was calculated by

$$\alpha = \arctan \frac{d_B - d_C}{BC} \quad (1)$$

where  $BC = 40$  mm.

A series of square wave voltage signals were generated via LabView (National Instruments), and amplified by power amplifiers then applied to the IPMC actuator. All signals have the same amplitude of 4 V but varying frequency from 0.1 Hz to 1 Hz. As mentioned earlier, IPMC actuator is used to generate thrust in underwater vehicles and so the kinematics were quantified in water. The fin was placed in a water tank and the laser sensors were fixed outside of the tank. Fig. 9 shows the experimental results at  $f = 0.2$  Hz. The upper figure shows the bending displacement  $d_B$ ,  $d_C$ , which indicates a delayed phase and an amplified magnitude between the bending motions at point B and C. The lower figure shows the calculated twist angle  $\alpha$ . The peak-to-peak twist angle is  $10^\circ$ , which is close to the angle generated by the pectoral fin in Chen and Tan [11]. Fig. 10 shows the plot of twist angle versus operating frequency. The maximum twist angle was generated at 0.2 Hz.

### Power consumption measurement

For applications such as an untethered bio-inspired robot, key questions regarding power consumption and optimal power management must be addressed. In this section, we study the

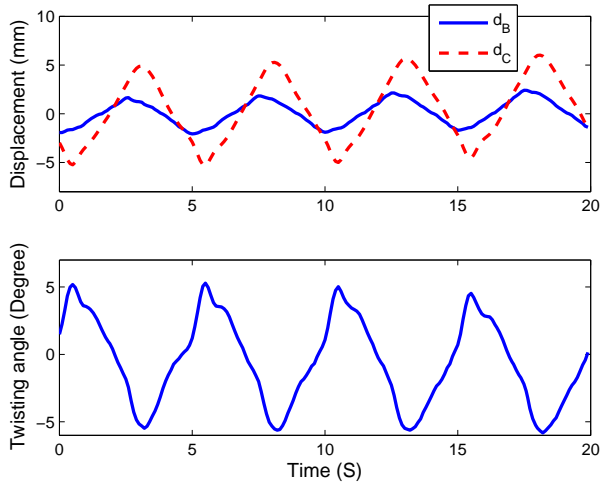


**FIGURE 9.** Bending displacements and twist angles under the actuation voltage (0.2 Hz, 4 V, square wave)

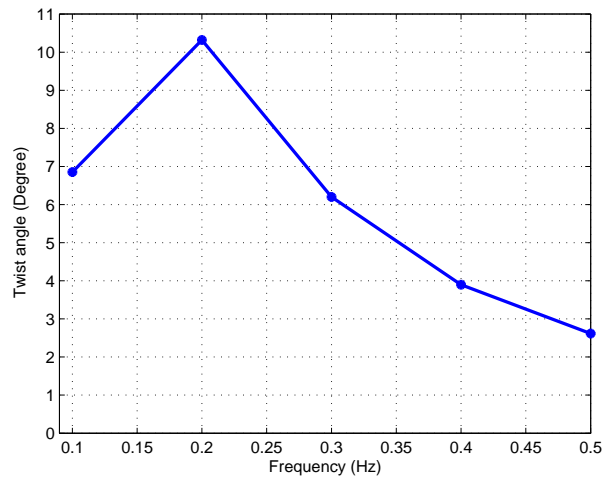


**FIGURE 10.** Peak-to-peak twist angle versus operating frequency

power consumption of the pectoral fin under a square wave actuation voltage because it is easy to be generated on board. The power consumed by the IPMC was calculated using the following equation:

$$P = \frac{1}{T} \int_0^T i(t)v(t)dt, \quad (2)$$

where  $i(t)$  and  $v(t)$  are measured actuation current and voltage, respectively, and  $T$  is the period of the actuation signal. A 3.5 V

and 0.2 Hz square wave voltage was applied to the IPMC of the pectoral fin, which was fixed inside the water tank. Fig. 11 shows the actuation voltage and current. To study the relationship between the power consumption and the operating frequency, a series of square wave actuation signals with an amplitude of 3.5 V and frequencies ranging from 0.1 Hz to 1 Hz were applied to the fin. Fig. 12 shows the power consumption versus operating frequency. It demonstrates that they are positively related and the power consumption at the cut-off frequency 0.3 Hz is 0.83 W.

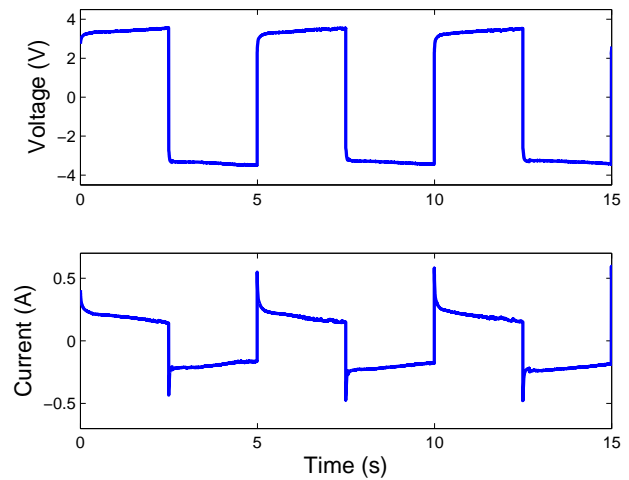


**FIGURE 11.** Actuation voltage and current measurement.

## DESIGN OF ROBOTIC COWNOSE RAY

In our previous work, a free swimming and IPMC enabled robotic manta ray was developed for the first time [13]. We used 4 IPMC beams bonded with thin PDMS membrane to create artificial pectoral fin. By independently controlling the bending of each IPMC beam, the fin can generate undulatory motions. However, in the free swimming test of the robot, only a flapping motion was generated due to the complexity of generating the four control signals on-board. Also the robot did not have a bio-inspired and waterproof body. In this paper, we present an IPMC-enabled robotic cownose ray capable of free swimming. It includes a on-board control unit, an bio-inspired and waterproof body, and two artificial pectoral fins. Since there is only one IPMC beam in the leading edge, one channel signal needs to be generated on-board, which simplifies the control strategy.

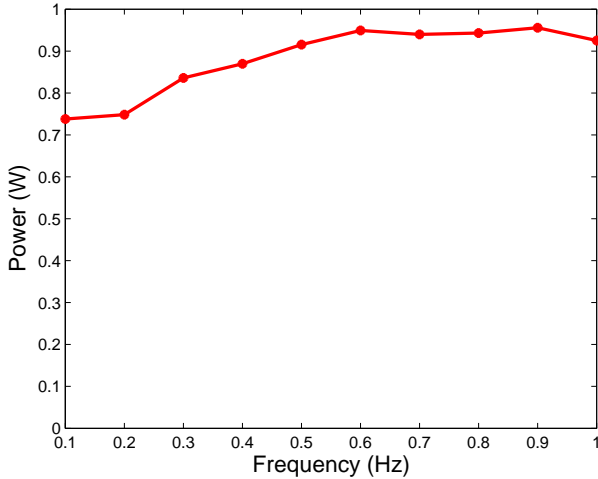


FIGURE 12. Power consumption versus operating frequency.

### On-board control circuit

The on-board circuit, which was developed in our previous work [13], provided a square wave voltage signal to the IPMC actuator in the pectoral fin. Fig 13(a) shows the schematic of the circuit. A 555-timer was used to generate a frequency tunable square wave. The amplitude of the voltage signal,  $V_p$ , was controlled by an adjustable voltage regulator. An H-bridge driver was used to draw up to 2 A output peak current. A rechargeable 7.3 V Lithium Ion Polymer battery (1700 mAh, AA Portable Power Corp) was selected as the power source for the robot. Fig. 13 (b) shows the picture of PCB board and battery.

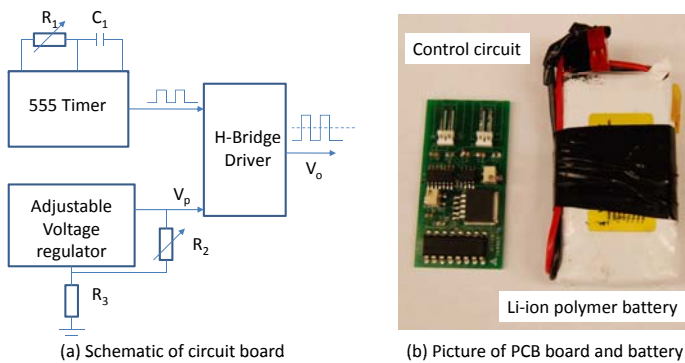


FIGURE 13. On board control unit [13].

### Bio-inspired Body Design

The robotic body was designed using Inventor (Autodesk). A set of CT Scan data from a biological cownose ray was used in the body design. The CT Scan data provided cross sectional images of the cownose ray's body. We took 10 cross sectional images of the center body and lofted them to create a 3-dimensional robotic body. Since a small scale robot was our interest, the robotic body was scaled down compared to that of the biological cownose ray. The overall the body dimensions were 21 cm long, 8.5 cm wide, and 5 cm thick (Fig. 14). The body consisted of a top part and a bottom part. In the bottom part, there was a cubic chamber to house the circuitry. In the top part, there was a O-ring that was used to seal the chamber to make the circuitry waterproof. Both parts had two gold electrodes that were used to apply electric signals to the IPMCs. The body was printed using a Fused Deposition Modeling (FDM) machine (uPrint Plus, Dimension). The fully assembled robot was 21 cm long, 33 cm wide, 5 cm thick, and weighted 119 grams. The free-swimming robot is shown in Fig. 15.

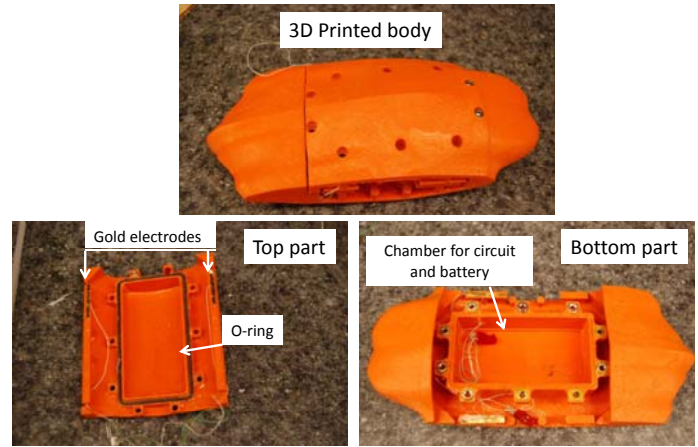
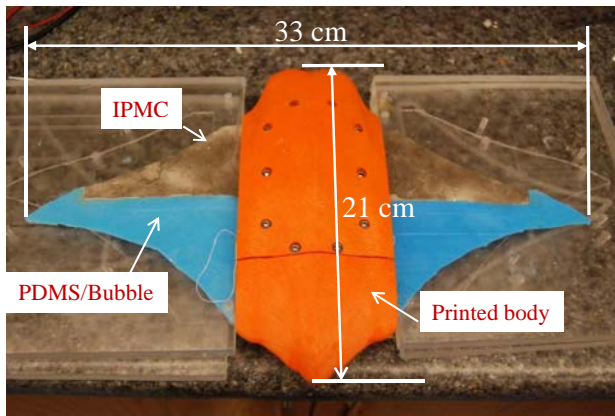


FIGURE 14. Bio-inspired robotic body.

### FREE SWIMMING TEST

The robot was tested in a water tank (1.5 m wide, 4.7 m long, and 0.9 m deep), which is shown in Fig. 16. The robot was neutrally buoyant underwater. The operating frequency of the square wave actuation voltage was tuned at 0.157 Hz and the amplitude was set at 3.3 V. A digital video camera (VIXIA HG21, Canon) was used to capture the videos of the swimming robot. Fig. 17 shows six snap shots of the swimming robot from top view. Each snap shot was taken every 5 second. The speed of the robot was extracted from the movie using the Edge Detection program in the Labview. The swimming speed shown in Fig. 17



**FIGURE 15.** Robotic cownose ray.

was 0.7 cm/s. Since the body length was 21 cm, the speed in body length per second was 0.034 BL/s.

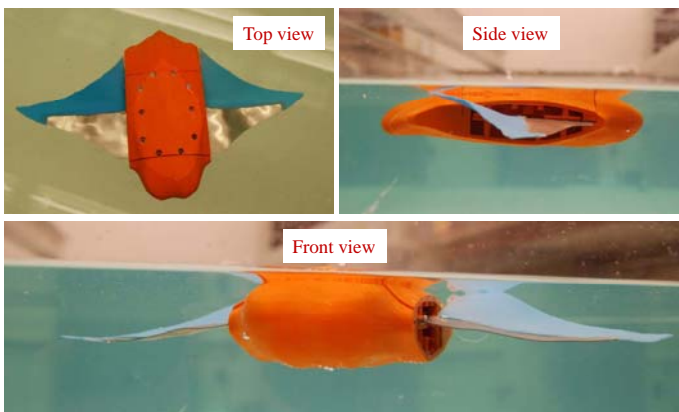


**FIGURE 16.** Pictures of the robot in underwater test.

## CONCLUSION AND FUTURE WORK

In this paper, a bio-inspired robotic cownose ray propelled by IPMC artificial pectoral fins has been developed. The artificial pectoral fin was fabricated by assembling IPMC actuator with a PDMS elastomer membrane. The fin was characterized in terms of tip deflection, twist angle, and power consumption. The characterization results have shown that the pectoral fin was able to generate up to 40% tip deflection and  $10^\circ$  twist angle with less than 1 Watt of power consumption. Based on the fabricated artificial fins, a small size and free swimming robotic cownose ray has been developed. Experimental results show that the robot

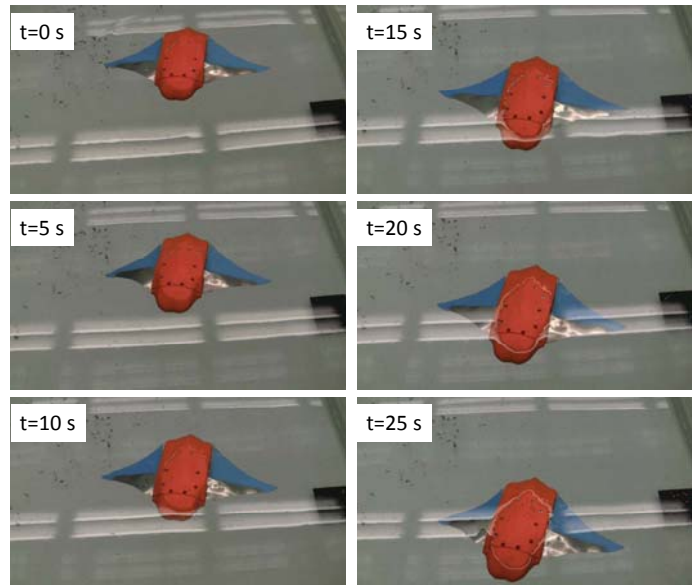


**FIGURE 17.** Snap shots of the free swimming robot.

swam at 0.034 BL/s. At this stage, the swimming speed of the robot is still low compared to the biological cownose ray.

In our future work, the propulsion efficiency of the robot will be studied, where the electrical to mechanical/fluid efficiency of the system will be calculated. We will improve the robot design in the following two aspects. First, kinematic and dynamic models of the cownose ray will be developed. It will help us to understand the propulsion mechanism of biological cownose ray and provide useful information on how to optimize the design and control of the pectoral fin. Second, an optimal design of the pectoral fin will be conducted to improve the propulsion efficiency.

## ACKNOWLEDGMENT

This research was supported in part by the Office of Naval Research (ONR) under the Multidisciplinary University Research Initiative (MURI) Grant N00014-08-1-0642 and the David and Lucille Packard Foundation. The authors would like to thank Mr. Robert Scott Russo for providing the CT Scan data of the cownose ray.

## REFERENCES

- [1] Rosenberger, L. J., 2001. "Pectoral fin locomotion in batooid fishes: Undulation versus oscillation". *The Journal of Experimental Biology*, **204**, pp. 379–394.
- [2] Moored, K., Smith, W., Hester, J., Chang, W., and Bart-Smith, H., 2008. "Investigating the thrust production of a

- myliobatoid-inspired oscillating wing". *Advances in Science and Technology*, **58**, pp. 25–30.
- [3] Moored, K., and Bart-Smith, H., 2009. "Investigation of clustered actuation in tensegrity structures". *International Journal of Solids and Structures*, **46**(17), August, pp. 3272–3281.
- [4] Guo, S., Fukuda, T., and Asaka, K., 2003. "A new type of fish-like underwater microrobot". *IEEE/ASME Transactions on Mechatronics*, **8**(1), pp. 136–141.
- [5] Punning, A., Anton, M., Kruusmaa, M., and Aabloo, A., 2004. "A biologically inspired ray-like underwater robot with electroactive polymer pectoral fins". In Proceedings of the 2004 IEEE International Conference on Mechatronics and Robotics, pp. 241–245.
- [6] Tan, X., Kim, D., Usher, N., Laboy, D., J.Jackson, A.Kapetanovic, Rapai, J., Sabadus, B., and Zhou, X., 2006. "An autonomous robotic fish for mobile sensing". In Proceedings of the IEEE/RSJ International Conference on Intelligent Robots and Systems, pp. 5424–5429.
- [7] Bar-Cohen, Y., 2000. "Electroactive polymers as artificial muscles - capabilities, potentials and challenges". In Handbook on Biomimetics, Y. Osada, ed., NTS Inc., pp. 1–13 (Chapter 8).
- [8] Shahinpoor, M., and Kim, K., 2001. "Ionic polymer-metal composites: I. Fundamentals". *Smart Materials and Structures*, **10**, pp. 819–833.
- [9] Kim, K. J., and Shahinpoor, M., 2003. "Ionic polymer-metal composites: II. manufacturing techniques". *Smart Materials and Structures*, **12**, pp. 65–79.
- [10] Chen, Z., and Tan, X., 2008. "A control-oriented and physics-based model for ionic polymer-metal composite actuators". *IEEE/ASME Transactions on Mechatronics*, **13**(5), pp. 519–529.
- [11] Chen, Z., and Tan, X., 2010. "Monolithic fabrication of ionic polymer-metal composite actuators capable of complex deformation". *Sensors and Actuators A: Physical*, **157**(2), pp. 246–257.
- [12] Anton, M., Punning, A., Aabloo, A., Listak, M., and Kruusmaa, M., 2004. "Towards a biomimetic EAP robot". In Proc. of Towards the Autonomous Mobile Robots, pp. 1–7.
- [13] Chen, Z., Um, T. I., and Bart-Smith, H., 2011. "A novel fabrication of ionic polymer-metal composite membrane actuator capable of 3-dimensional kinematic motions". *Sensors and Actuators A: Physical*, **168**(1), pp. pp 131–139.
- [14] Kim, K. J., and Shahinpoor, M., 2002. "A novel method of manufacturing three-dimensional ionic polymer-metal composites (IPMCs) biomimetic sensors, actuators, and artificial muscles". *Polymer*, **43**, November, pp. 797–802.
- [15] Kim, S. J., Lee, I. T., and Kim, Y. H., 2007. "Performance enhancement of IPMC actuator by plasma surface treatment". *Smart Materials and Structures*, **16**(1), January, pp. N6–N11.
- [16] Chung, C., Fung, P., Hong, Y., Ju, M., Lin, C., and Wu, T., 2006. "A novel fabrication of ionic polymer-metal composites (IPMC) actuator with silver nano-powders". *Sensors and Actuators B: Chemical*, **117**, November, pp. 367–375.
- [17] Lee, S. J., Han, M. J., JunKim, S., Jho, J., Lee, H. Y., and Kim, Y. H., 2006. "A new fabrication method for IPMC actuators and application to artificial fingers". *Smart Materials and Structures*, **15**(5), August, pp. 1217–1224.
- [18] Nemat-Nasser, S., and Li, J., 2000. "Electromechanical response of ionic polymer-metal composites". *Journal of Applied Physics*, **87**(7), pp. 3321–3331.
- [19] Chen, Z., Sharata, S., and Tan, X., 2010. "Modeling of biomimetic robotic fish propelled by an ionic polymer metal composite caudal fin". *IEEE/ASME Transactions on Mechatronics*, **15**(3), pp. 448–459.